Title	Liquid-phase monolayer doping of InGaAs with Si-, S-, and Sn-containing organic molecular layers
Authors	O'Connell, John;Napolitani, Enrico;Impellizzeri, Giuliana;Glynn, Colm;McGlacken, Gerard P.;O'Dwyer, Colm;Duffy, Ray;Holmes, Justin D.
Publication date	2017-05-01
Original Citation	O'Connell, J., Napolitani, E., Impellizzeri, G., Glynn, C., McGlacken, G. P., O'Dwyer, C., Duffy, R. and Holmes, J. D. (2017) 'Liquid-Phase Monolayer Doping of InGaAs with Si-, S-, and Sn-Containing Organic Molecular Layers', ACS Omega, 2(5), pp. 1750-1759. doi: 10.1021/acsomega.7b00204
Type of publication	Article (peer-reviewed)
Link to publisher's version	10.1021/acsomega.7b00204
Rights	© 2017 American Chemical Society. This is an open access article published under an ACS AuthorChoice License, which permits copying and redistribution of the article or any adaptations for non-commercial purposes. - http://pubs.acs.org/page/policy/authorchoice_termsofuse.html
Download date	2024-05-07 12:18:35
Item downloaded from	https://hdl.handle.net/10468/3910

ACS OMEGA

Article

http://pubs.acs.org/journal/acsodf

Liquid-Phase Monolayer Doping of InGaAs with Si-, S-, and Sn-Containing Organic Molecular Layers

John O'Connell,[†,‡,§] Enrico Napolitani,[∥,⊥] Giuliana Impellizzeri,[⊥] Colm Glynn,[†,‡] Gerard P. McGlacken,[†] Colm O'Dwyer,[†,‡] Ray Duffy,[‡] and Justin D. Holmes*[,†,‡,§]

[†]Department of Chemistry and [‡]Tyndall National Institute, University College Cork, Cork, Ireland

[§]AMBER@CRANN, Trinity College Dublin, Dublin 2, Ireland

[∥]Dipartimento di Fisica e Astronomia, Università di Padova, Via Marzolo 8, I-35131 Padova, Italy

[⊥]CNR-IMM, Via S. Sofia 64, 95123 Catania, Italy

S *Supporting Information*

ABSTRACT: The functionalization and subsequent monolayer doping of InGaAs substrates using a tin-containing molecule and a compound containing both silicon and sulfur was investigated. Epitaxial InGaAs layers were grown on semi-insulating InP wafers and functionalized with both sulfur and silicon using mercaptopropyltriethoxysilane and with tin using allyltributylstannane. The functionalized surfaces were characterized using X-ray photoelectron spectroscopy (XPS). The surfaces were capped and subjected to rapid thermal annealing to cause in-diffusion of dopant atoms. Dopant diffusion was monitored using secondary ion mass spectrometry. Raman scattering was utilized to nondestructively determine the presence of dopant atoms, prior to destructive analysis, by comparison to a blank undoped sample. Additionally, due to the As-dominant surface chemistry, the resistance of the functionalized surfaces to oxidation in ambient conditions over periods of 24 h and 1 week was elucidated using XPS by monitoring the As 3d core level for the presence of oxide components.

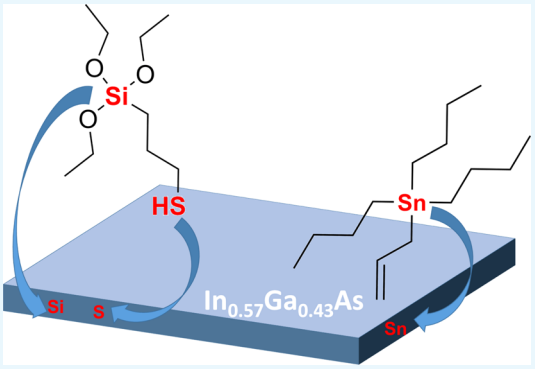

INTRODUCTION

InGaAs is a promising potential future channel material for complementary metal-oxide semiconductor (CMOS) applications due to its direct band gap and high electron mobility.[1−6] With device feature sizes perennially decreasing and a move away from SiO_2-based gate dielectric strategies ongoing, new methods for passivating and doping of InGaAs based materials will become more important if the material is to become integrated in future technology nodes. Metal-oxide semiconductor field-effect transistors (MOSFETs) based on InGaAs will allow continued scaling through a reduction in operation voltage and device footprints without compromising performance. Source and drain (S/D) doped III−V MOSFET devices are still attracting considerable attention. Advanced III−V-based CMOS processes and technologies require ultrathin body channel materials to maintain minimal junction and gate leakage and to reduce short channel effects. S/D regions with increased thickness will also be required to further reduce access resistances. Si and Sn are typical dopants of choice for n-type doping of InGaAs. Doping of InGaAs conventionally takes place either in situ by introducing a dopant-containing gas during epilayer growth, by ion implantation post growth, or in the case of a device such as a MOSFET, selective epitaxy on each side of the gate of in situ doped source/drain materials using the channel material as a seed layer. Typically, the highest temperature step for an InGaAs MOSFET fabrication process approaches 550 °C. From a device fabrication perspective, it is desirable to reduce the thermal budget as much as possible, whilst maintaining high carrier concentrations. For this reason, Sn is the preferred n-type dopant at such temperatures, as active carrier concentrations above 5×10^{19} atoms cm^{-3} can potentially be achieved for relatively low epitaxy thermal parameters.[7] However, Si doping may still be more desirable due to its compatibility with front-end CMOS processes. More pertinently, the limited diffusivity of Si in InGaAs would prove beneficial if high-concentration, ultrashallow junctions are to be realized, especially in the case of nanostructures.

Conformal doping of nanostructures becomes challenging, especially for three-dimensional structures, as dimensions are scaled down. Established methods for doping, such as ion implantation, suffer from several drawbacks at the nanoscale, such as stochastic dopant distributions, the inability to control the abruptness to within a nanometer, and most importantly at the nanoscale, beam-induced damage in the case of devices. Furthermore, ion implant damage in III−V materials is generally considered difficult to repair, even with prolonged

Received: February 21, 2017
Accepted: April 17, 2017
Published: May 1, 2017

DOI: 10.1021/acsomega.7b00204
ACS Omega 2017, 2, 1750−1759

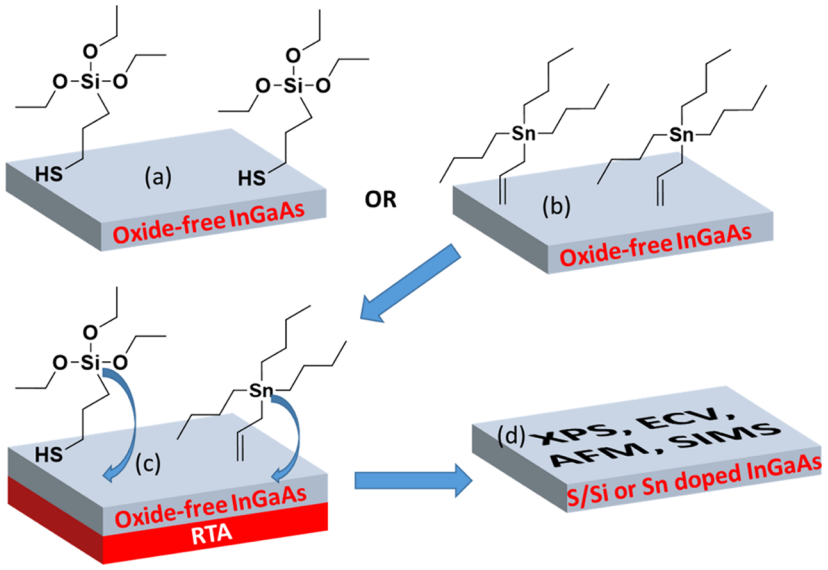

Figure 1. General schematic for the InGaAs MLD process: (a) an oxide-free InGaAs surface was functionalized with 3-mercaptotriethoxysilane (MPTES) or (b) allyltributylstannane (ATBS). (c) The functionalized substrates were capped with SiO_2 and annealed in a rapid thermal anneal furnace to cause in-diffusion of the dopant atoms to yield (d) doped InGaAs substrates.

annealing. Monolayer doping (MLD), a technique to controllably dope semiconductor surfaces and nanostructures at shallow depths, has been applied successfully to Si and Ge using a range of functionalization and dopant synthesis strategies. A typical MLD process combines the rich surface chemistry of semiconductors[8−11] with the self-assembly of dopant-containing molecules on a semiconductor surface. This surface is then capped, to prevent desorption of the chemisorbed monolayer, and annealed using a rapid thermal anneal process to yield shallow, high-concentration dopant profiles. MLD has already been shown to be a suitable technique for the shallow doping of Si and Ge devices with complex and nonplanar geometries, allowing fine control over dopant profiles.[12−30]

The functionalization of semiconductor surfaces can also enhance the resistance of these surfaces toward oxidation. Due to the challenging surface chemistry of InGaAs and other III−V materials, the application of MLD has been quite limited. There have been reports of direct bonding to oxide-free III−V surfaces using organic thiols,[31−35] and due to the simplicity of the procedure and availability of suitable commercial molecules, as well as the excellent oxidation resistance offered by III−V-thiol chemistry, this was one of the functionalization approaches used in this study. Solution-phase S doping of InGaAs has been relatively widely reported due to the simplicity of the procedure.[36−39] Ammonium sulfide is often used to remove the native oxides on InGaAs, but the process conveniently results in a S-terminated surface, allowing diffusion of S as a monolayer into the InGaAs surface via a rapid thermal anneal step. Although not a traditional MLD process, due to the gas-phase nature of the dopant precursor and high-vacuum requirements of the deposition process, Kong and co-workers recently reported the Si MLD of InGaAs nanostructures by means of a MOCVD-deposited silane layer with a thickness of a few monolayers.[40] Enabling precision control over dopant profiles in III−V materials remains a challenge to be overcome if the high carrier mobilities are to be exploited in highly-scaled device architectures.

In this article, we report for the first time, the functionalization of epitaxially grown InGaAs layers, using a typical ambient pressure, liquid-phase MLD procedure, with a Si- and S-containing thiol and with a Sn-containing organometallic molecule. The decision to use a molecule containing both Si and S was taken to not only have the benefit of two dopant atoms in one molecule but also to take advantage of well-known III−V-thiol surface chemistry to minimize oxidation by ambient conditions. Surface chemistry on the functionalized InGaAs surface was characterized using XPS. The presence of dopants in the processed samples was nondestructively ascertained by means of Raman scattering. Dopant diffusion was monitored using secondary ion mass spectrometry (SIMS) to measure the total chemical concentration of the dopants. A schematic illustrating the chemical functionalization process is shown in Figure 1.

EXPERIMENTAL SECTION

All reagents were purchased from Sigma-Aldrich and used as received, unless specified. All chemical manipulations were carried out under strictly inert conditions in an atmosphere of ultrahigh purity argon from Air Products Inc., in an Innovative Technologies inert-atmosphere glovebox and on Schlenk apparatus.

XPS Characterization. XPS spectra were acquired on an Oxford Applied Research Escabase XPS system equipped with a CLASS VM 100 mm mean radius hemispherical electron energy analyzer with a three-channel detector arrangement in an analysis chamber with a base pressure of 10×10^{-10} mbar. Survey scans were acquired between 0 and 1400 eV with a step size of 0.7 eV, dwell time of 0.5 s and pass energy of 100 eV. Core-level scans were acquired at the applicable binding energy range for each core level, with a step size of 0.1 eV, dwell time of 0.05 s and pass energy of 20 eV averaged over 100 scans. To ensure a good signal-to-noise ratio, the Sn 3d core-level scans were averaged over 200 scans. An Al Kα X-ray source at 200 W power was used for all scans. Multiplier voltage was maintained at 2.2 kV for all acquisitions. All spectra were acquired at a take-off angle of 90° with respect to the analyzer axis and were

DOI: 10.1021/acsomega.7b00204
ACS Omega 2017, 2, 1750−1759

charge corrected with respect to the C 1s photoelectric line by rigidly shifting the binding energy scale to 285 eV. Data were processed using CasaXPS software, whereby a Shirley background correction was employed and peaks were fitted to Voigt profiles. To ensure accurate quantification, atomic sensitivity factors were taken from the data acquisition software and manually input into the data processing software.

SIMS Profiling. Samples doped with Si and S were analyzed with a Cs^+ primary beam with 7.25 keV acceleration voltage and 65 nA beam current, rastered over an area of 250 × 250 μm^2. $^{75}As^-$, $^{30}Si^-$, and $^{32}S^-$ ions were collected from each sample during sputtering from a central area of approximately 60 μm in diameter. Sn doped samples were analyzed with a O_2^+ primary beam with 3 keV acceleration voltage and 200 nA beam current, rastered over an area of 250 × 250 μm^2. $^{120}Sn^+$ and $^{75}As^+$ secondary ions were collected during sputtering from a central area of approximately 150 μm in diameter. Ion-implanted standards for the calibration of the SIMS concentration were prepared for Sn, Si, and S by implanting $^{120}Sn^+$ at 180 keV with a fluence of 1.7×10^{14} ions cm^{-2}, $^{30}Si^+$ at 50 keV with a fluence of 4×10^{14} ions cm^{-2}, and $^{32}S^+$ at 60 keV with a fluence of 4×10^{14} ions cm^{-2}, respectively. The substrates were held at room temperature during the implantation process. The ion beams were oriented by 7° to the normal of the wafer surface to avoid channeling effects. Although C may have an effect on junction leakage, it was not studied in this work due to it being only problematic for fabrication of very lightly-doped InGaAs thin films. The dopant-containing molecules were chosen as their small size aims to minimize the amount of C on the surface. Depth calibration was performed by measuring the SIMS crater depth using a profilometer and by assuming a uniform erosion rate in the InGaAs layers. Further details on the SIMS analysis and preparation of the ion-implanted standards are available in the Supporting Information.

Raman Scattering. Raman scattering data were collected with a Renishaw InVia Raman spectrometer equipped with a 2400 lines/mm grating using a 514 nm 30 mW argon ion laser. Spectra were collected using a RenCam CCD camera. The beam was focused onto samples using either a 20× or a 50× objective lens. The laser power density was adjusted to ensure that the thin film surfaces did not undergo sample heating during the full spectral acquisition time. Although in principle, Raman spectroscopy may be able to provide a measure of substitutional versus nonsubstitutional atoms, this would require much more advanced instrumentation, therefore, efforts were focused on utilizing Raman scattering to nondestructively analyze the samples for the presence of dopants prior to SIMS analysis.

InGaAs Sample Fabrication. Epitaxial $In_{0.57}Ga_{0.43}As$ semiconductor layers with an approximate thickness of 200 nm were grown on 2 inch semi-insulating InP substrates using an Aixtron metal−organic vapor phase epitaxy (MOVPE) system. Trimethylindium, trimethylgallium, and arsine were used as the In, Ga, and As sources, respectively. An AlInAs barrier of approximately 100 nm was grown on the InP substrate prior to epitaxy of InGaAs to prevent upward diffusion of dopant atoms from the InP substrates during the rapid thermal anneal step, thus negating the effect of the substrate on any measurements. This stack structure minimizes defects at this composition due to nominal lattice matching between each of the layers. A schematic showing the stack structure is shown in Figure S1.

General Procedure for the Functionalization of the InGaAs Surface with 3-Mercaptotriethoxysilane. All glassware was cleaned scrupulously with Alconox detergent followed by copious rinsing with water and then cleaned with a piranha wash (CAUTION: this is a strong oxidizing agent and reacts violently with organic substances), dried in an oven overnight at 130 °C, and allowed to cool under a stream of dry Ar on the Schlenk line. InGaAs substrates were cleaved into 1 × 1 cm^2 pieces. Samples were prepared for functionalization using procedures adapted from McGuiness et al.[41] Briefly, the InGaAs token was degreased by sonication in acetone, MeOH, and isopropyl alcohol (IPA) for 15 min in each solvent and dried in a N_2 stream. The substrate was then dipped in a concentrated ammonium hydroxide solution for 2 min to remove the native oxides, rinsed in anhydrous IPA, and dried in a N_2 stream. The substrate was then immediately placed into a two-necked round bottom flask under a positive pressure of Ar with one arm connected to the Schlenk line and the other neck stoppered. In a separate Schlenk flask, a 25% v/v solution of 3-mercaptotriethoxysilane in anhydrous IPA was dried and degassed using four freeze−pump−thaw cycles. The solution was cannulated under a positive pressure of Ar into the flask containing the oxide-free InGaAs substrate and was left for 17−24 h at 80 °C. The substrate was then rinsed using hot IPA to remove physisorbed species and was immediately placed into an inert atmosphere prior to characterization.

General Procedure for the Functionalization of the InGaAs Surface with ATBS. Glassware was cleaned as described previously. Samples were prepared for functionalization using procedures adapted from Lie and co-workers.[42] InGaAs substrates were cleaved into 1 × 1 cm^2 pieces. The InGaAs token was degreased by sonication in methanol and acetone for 5 min each followed by drying in a stream of ultrapure N_2. Native oxide removal was performed in hydrofluoric acid and water. The liquid-phase HF etching of the InGaAs token took place in an aqueous solution of HF (49%, Honeywell) and ultrapure water (UPW, Milli-Q, 18 MΩ cm^{-1}) at a volumetric ratio of 1:50 for 5 min at room temperature. The sample was rinsed with UPW and dried in an ultrapure N_2 stream. These etching parameters have been reported to give an As-rich surface containing As−As or As−H bonds.[42] ATBS was dissolved in previously distilled and dried mesitylene to make up a 25% v/v solution in a Schlenk flask. This flask was subjected to three freeze−pump−thaw cycles to remove any dissolved gases. This solution was cannulated directly under positive pressure of Ar into a flask containing the InGaAs token. The reaction vessel was heated to 160 °C to maintain reflux and left for 2 h. The sample was rinsed consecutively in anhydrous toluene, hexane, ethanol, and a final rinse in toluene to remove any physisorbed species. All samples were kept under an inert atmosphere prior to characterization and processing.

RESULTS AND DISCUSSION

Modification of the Oxide-Free InGaAs Surface with 3-Mercaptopropyltriethoxysilane (MPTES). Si is one of the most popular dopants for InGaAs, especially when introduced via ion implantation and in situ growth. Significantly, Si has a sticking coefficient approaching unity and very low diffusivity making the doping of InGaAs using Si attractive for devices that require high doping concentrations and sharp, shallow doping profiles. However, Si exhibits amphoteric behavior in InGaAs leading to complications in determining active carrier

DOI: 10.1021/acsomega.7b00204
ACS Omega 2017, 2, 1750−1759

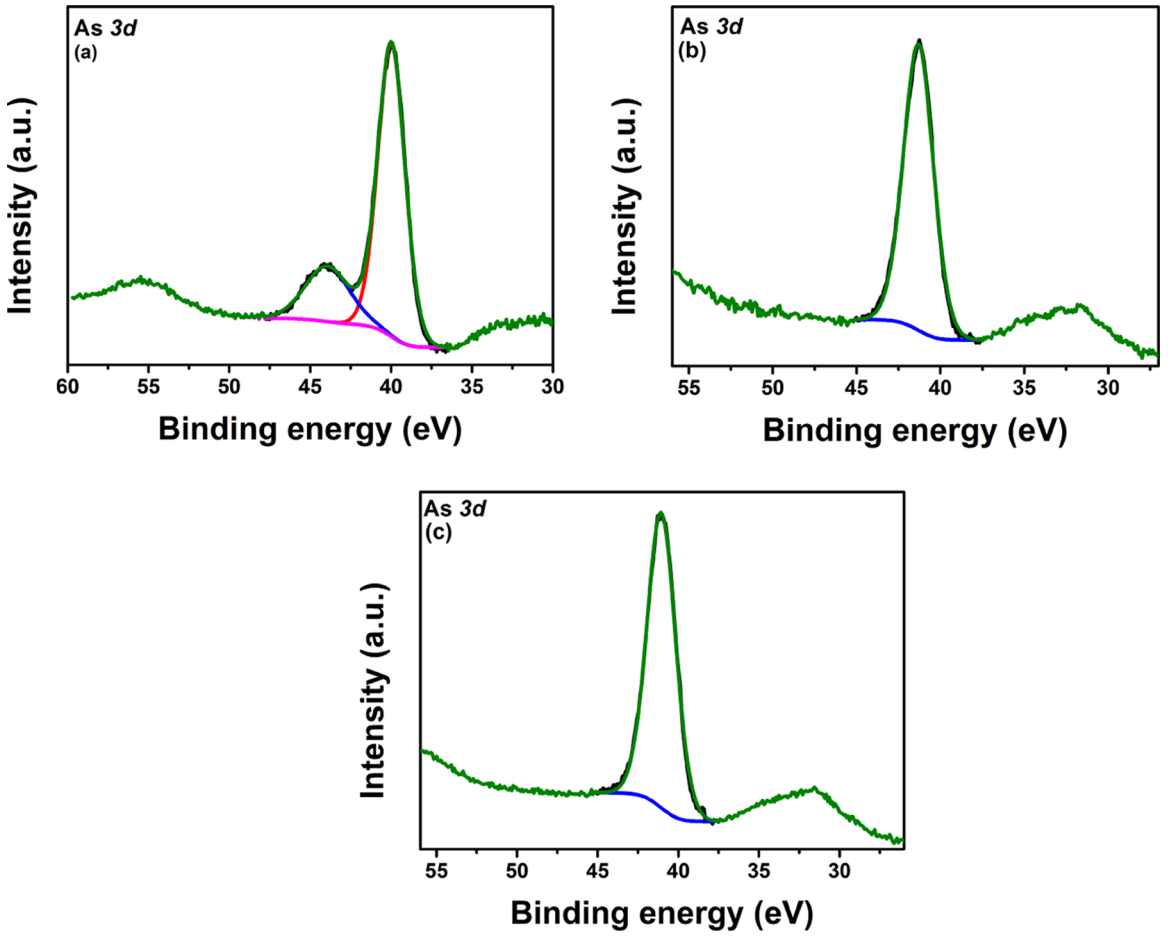

Figure 2. XPS spectra of the As 3d core level depicting the surface chemistry for: (a) an as-received InGaAs substrate, (b) an InGaAs substrate freshly etched with ammonium hydroxide, and (c) an InGaAs substrate functionalized with MPTES. The large oxide component present at 44 eV in (a) disappears after the ammonium hydroxide etch and remains absent in the functionalized substrate, highlighting that the functionalization process did not increase the amount of As oxides on the surface.

concentrations as Si can act as both an n-type and p-type dopant.[43] Hence, the concentration of conducting electrons is typically lower than the number of silicon dopant atoms and it is challenging to achieve free carrier concentrations in the 10^{19} range. XPS characterization was conducted on all samples to determine if MPTES chemisorbed on the surface of InGaAs, thereby indicating successful functionalization, and also to investigate whether or not the sample oxidized during the functionalization process. Each sample was sonicated in anhydrous ethanol prior to insertion into the UHV atmosphere of the XPS spectrometer to remove physisorbed species. Figure 2 shows the As 3d core-level spectra for (a) an as received, cleaved InGaAs wafer, (b) an oxide-free InGaAs wafer, and (c) an oxide-free InGaAs surface that has been functionalized with the MPTES molecule. Figure 2a shows primarily a peak at 40 eV, which is indicative of unoxidized elemental As from InGaAs.[44] A shoulder peak chemically shifted to approximately 44 eV is present, which is representative of oxidized arsenic species.[45] Shown in Figure 2b is an XPS spectrum of the same sample analyzed immediately after an NH_4OH etch to remove the native oxides. The spectrum is dominated solely by the elemental arsenic peak, showing effective native oxide removal at the surface. Figure 2c shows an XPS spectrum of the same sample after immersion in a 25% v/v solution of MPTES in IPA for 24 h. The spectrum exhibits only a peak at 40 eV showing the presence of nonoxidized As as part of an oxide-free InGaAs surface. This shows that despite the long substrate immersion times, no oxide had regrown on the surface postfunctionalization. Figure S2 shows the survey spectra for the as-received wafers, oxide-free wafers, and samples that have been functionalized with the MPTES molecule.

Figure 3a shows the combined XPS As 3p, S 2p, and Ga 3s core-level scans of the MPTES-functionalized substrate. The component at approximately 161 eV can tentatively be attributed to the presence of S in a thiolate form, which would be consistent with direct S-substrate bonding of the MPTES molecule.[46] Instrumental resolution was limited in the experiments due to the use of a nonmonochromated X-ray source which precludes further resolution of this thiolate peak to determine if the bonding mode is Ga−S or As−S. Nevertheless, the presence of S on the surface after copious postreaction washing would imply that the MPTES molecule has successfully bonded covalently to the oxide-free InGaAs surface. Figure 3b shows the C 1s core-level scan of the MPTES-functionalized surface. The main component shown in red at 285 eV represents a combination of adventitiously bound carbon as well as C−C moieties from the MPTES molecule. The smaller blue component located at approximately 287 eV is indicative of C−O/C−S moieties, which are also consistent with the structure of the MPTES molecule. Due to overlap of the S 2p and Ga 3s regions shown in (b), it is nontrivial to compare the peak intensities to the C 1s peak to elucidate

DOI: 10.1021/acsomega.7b00204
ACS Omega 2017, 2, 1750−1759

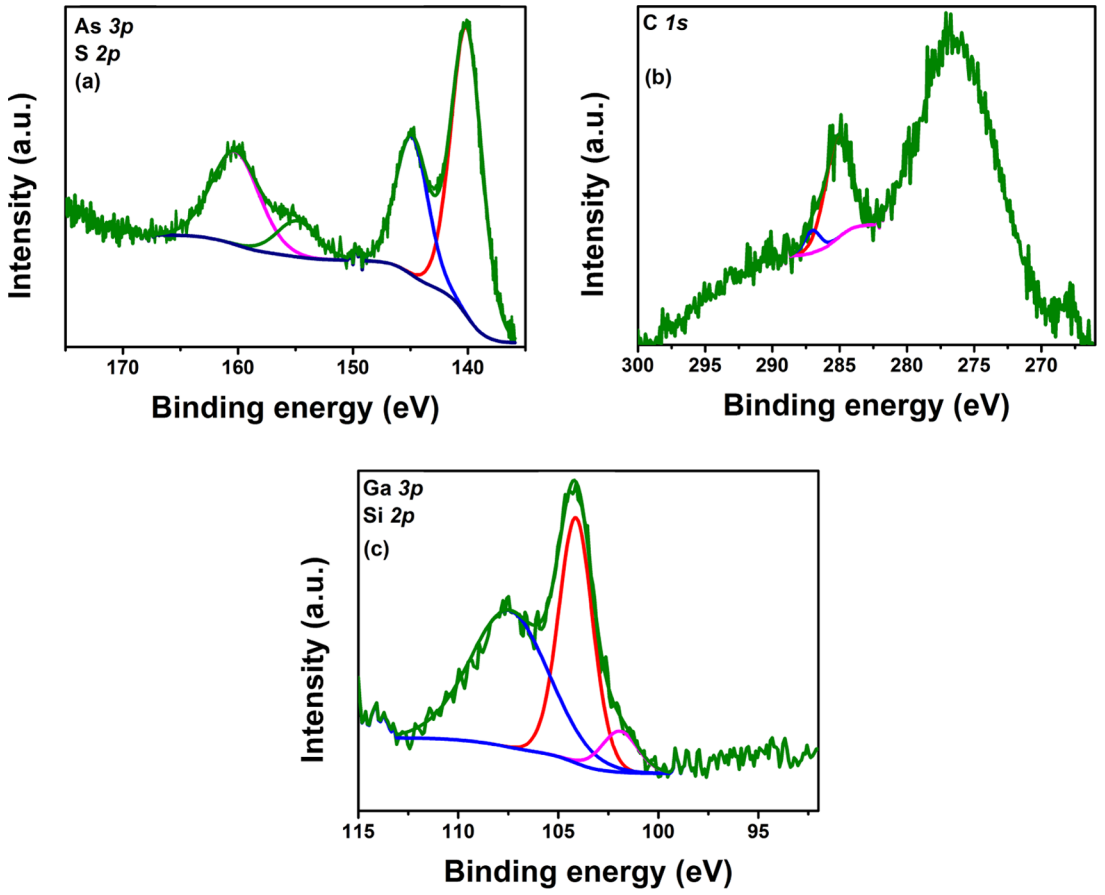

Figure 3. (a) Combined As 3p, S 2p, and Ga 3s core-level XPS spectra showing the presence of S on the surface with (b) showing the C 1s peak with C−O/S chemical moieties indicated by the blue peak and (c) combined Ga 3p and Si 2p core-level scans. A small shoulder peak in (c), indicated in pink, shows tentative evidence for the presence of Si on the surface from the MPTES molecule.

rudimentary film-thickness measurements. This overlap also makes the estimation of molecular packing densities extremely difficult. Nonetheless, with copious postreaction washing of the substrates, all physisorbed material is likely to be removed leaving only the chemisorbed monolayer. Figure 3c shows the combined scan for the Ga 3p and Si 2p regions. Again, due to the complex XPS spectra with regard to peak overlaps and surface plasmons, it is nontrivial to determine the presence of Si. A shoulder located at approximately 101 eV, attributed to the Si 2p peak, could tentatively be fitted. Attempts were made to fit the peak with and without this shoulder. The peak fit remained better with the shoulder peak present, showing the presence of Si could cautiously be confirmed. Combined with the data showing the presence of S, the chemisorption of the MPTES molecule was deemed successful.

Dopant Characterization of InGaAs Surfaces Functionalized with 3-MPTES and Subsequently Capped and Treated with a Rapid Thermal Anneal. Samples functionalized with MPTES were removed from an inert atmosphere and capped with 50 nm of sputtered SiO_2 and heated in a rapid thermal anneal furnace to 700 and 750 °C for 10 and 20 s under nitrogen. Although the choice of method for the capping layer deposition and the specific composition of the capping layer may affect the monolayer integrity, these effects were not studied in this work. The choice of capping layer can also dictate whether the dopant molecules diffuse upwards into the capping layer or down into the semiconductor substrate intended for doping, that is, dopant segregation. Dopant segregation coefficients are widely known for dopants such as P and B for doping of Si with SiO_2 capping layers. However, to the best of our knowledge, literature on the segregation coefficients for S, Si, and Sn for an InGaAs/SiO_2 system is scarce, especially for species diffusing from the semiconductor surface. Plasma-enhanced chemical vapor deposition, electron-beam evaporation, or spin-coating could be used to deposit the capping layer to determine the effect, if any, on the MLD process. Following the anneal step, a buffered-oxide etch was used to remove the oxide prior to dopant characterization. Raman scattering was utilized in the first instance to "fingerprint" the samples nondestructively for the presence of dopants prior to destructive SIMS analysis. Raman scattering has been used as a noncontact method to elucidate carrier density, crystallinity, and band-bending in binary and ternary III−V semiconductors.[47,48] Data obtained for MPTES-functionalized samples which were subjected to a rapid thermal anneal process at different temperatures are shown in Figure S3. As can be seen from the peak intensity reduction and shift, when compared to that of a bulk, undoped sample, the dopant introduction has an effect on the Raman signature of the InGaAs, suggesting an alteration in the structure. Due to the bulk nature of the material, no damage caused by the laser beam was observed on the surface of the sample, showing the change in the Raman signature is due to dopant incorporation, as opposed to thermal stress caused by the laser power. A lower laser power of 50% was used as a precaution. Electrochemical capacitance−voltage measurements cannot differentiate be-

DOI: 10.1021/acsomega.7b00204
ACS Omega 2017, 2, 1750−1759

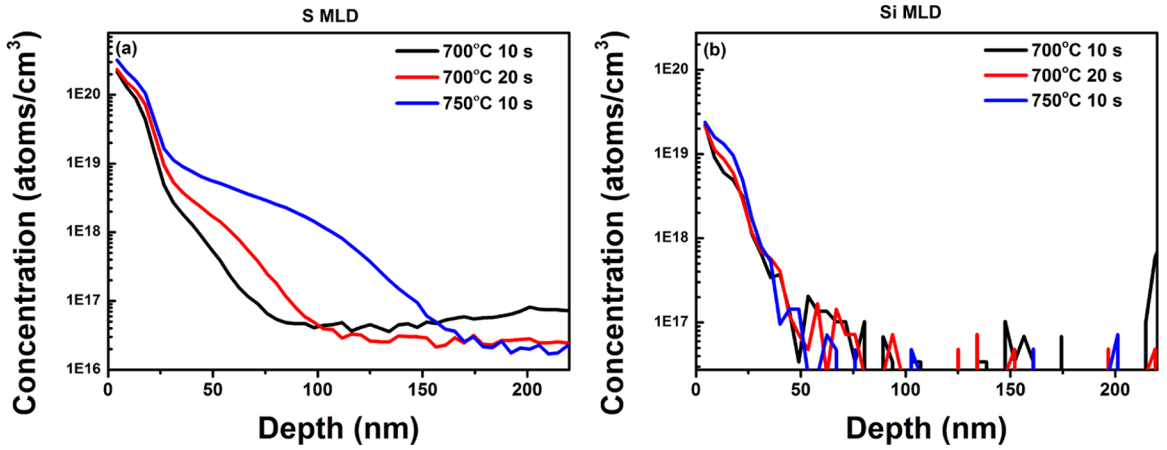

Figure 4. SIMS profiles showing: (a) sulfur concentration vs depth and (b) silicon concentration vs depth data for MPTES-functionalized samples which were subjected to a capping step and rapid thermal anneal process. The sample annealed at 700 °C for 10 s exhibited a peak S concentration of approximately 2×10^{20} atoms/cm^3 with a maximum junction depth of approximately 75 nm. A sample annealed at 700 °C for a longer time of 20 s exhibited a similar concentration approaching 3×10^{20} atoms/cm^3. A sample functionalized with MPTES and then subjected to an anneal at a higher temperature of 750 °C for 10 s exhibited a slightly higher peak concentration approaching 4×10^{20} atoms/cm^3. (b) The sample annealed at 700 °C for 10 s exhibited a peak Si concentration of approximately 1×10^{19} atoms/cm^3 with a maximum junction depth of approximately 50 nm. A sample annealed at 700 °C for a longer time of 20 s exhibited a similar concentration approaching 1×10^{19} atoms/cm^3 with a similar junction depth of approximately 50 nm. A sample functionalized with MPTES and then subjected to an anneal at a higher temperature of 750 °C for 10 s exhibited a very similar profile to the previous Si profiles, giving a maximum concentration of approximately 1×10^{19} atoms/cm^3 with a relatively shallow junction depth of approximately 50 nm.

tween S and Si to give active carrier concentration data. Thus, SIMS was the analysis method of choice for dopant profile analysis. Figure 4a displays a SIMS profile showing sulfur concentration versus depth data for the MPTES-functionalized samples which were subjected to a capping step and rapid thermal anneal process. The sample annealed at 700 °C for 10 s exhibited a peak carrier concentration of approximately 2×10^{20} atoms/cm^3 with a maximum junction depth of approximately 75 nm. Another MPTES sample functionalized similarly and annealed at 700 °C for a longer time of 20 s exhibited a similar concentration approaching 2×10^{20} atoms/cm^3 with an approximate increase of 25 nm in the junction depth to 100 nm. A sample functionalized with MPTES and then subjected to an anneal at a higher temperature of 750 °C at 10 s exhibited a slightly higher peak concentration approaching 4×10^{20} atoms/cm^3. Additionally, the dopant profile at the higher anneal temperature was much deeper, with a maximum junction depth of 150 nm for the S-MLD process. The data shown in Figure 4b show Si concentration versus depth data collected simultaneously with the S data on the same samples as shown in Figure 4a. Due to the differing diffusivity of Si versus S in InGaAs, Si does not diffuse as well as S. The concentrations of Si when compared to the concentrations of S were generally an order of magnitude lower. All three samples exhibited very similar profiles in terms of peak concentrations at approximately 1×10^{19} atoms/cm^3. This unusual phenomenon, whereby the concentration of Si saturates, has been observed previously and several models exist to explain the saturation of Si doping in III−V materials. The low solubility of n-type dopants in InGaAs, such as Si, is a significant barrier to the creation of low-resistance S/D regions in devices, in addition to impeding the fabrication of ohmic contacts. This lack of temperature dependence for Si solubility has been studied in detail for Si-implanted InGaAs susbstrates,[49,50] but further work will be needed to fully understand the diffusion mechanism from an MLD perspective, that is, diffusion from the surface.

Despite the difficulty in characterizing the Si-doped samples, we have shown that it is possible to co-dope InGaAs with S and Si simultaneously using liquid-phase, ambient pressure surface chemistry. However, the junction depths are quite deep highlighting the need for more advanced annealing techniques with faster ramp up and ramp down rates in addition to emerging techniques such as flashlamp and laser annealing.[51−54]

Modification of the Oxide-Free InGaAs Surface with ATBS. Sn is a widely used group IV dopant for the preparation of n-type InGaAs layers, especially in molecular beam epitaxy. Unlike Si and Ge, Sn does not exhibit amphoteric behavior in InGaAs and will act as an n-type dopant only. Thus, Sn is the dopant of choice to achieve heavily n-doped III−V materials. Unfortunately, suitable Sn precursors for MLD are scarce due to the complex InGaAs surface chemistry. Following the cleaning and etching procedure developed by Lie et al.,[42] an As-dominant surface results, which, following a DI water rinse, leaves a H-terminated surface that may be reacted with the labile C═C site on ATBS. The presence of inorganic fluorides, typically observed by XPS in the F 1s region at approximately 690 eV postclean would indicate an incomplete cleaning process, but XPS analysis did not show evidence for the formation of such fluorides. Figure 5 shows a Sn 3d core-level spectrum of an InGaAs surface that has been functionalized with the ATBS molecule. The spectrum is dominated by the Sn 3d elemental doublet. The doublet separation is approximately 8.3 eV, which would indicate oxidation of the monolayer, which is consistent with instability of the organostannane in air. Samples were prepared to monitor the stability of the underlying substrate toward reoxidation. The XPS survey spectra for the as received and cleaned substrates used for the ATBS functionalization are shown in Figure S4. Attempts were made to probe the nature of the bond between the ATBS molecule and the oxide-free InGaAs surface using FTIR. The signal for the As−C bonding modes was indiscernible from noise during the analysis. The presence of Sn on the surface via

DOI: 10.1021/acsomega.7b00204
ACS Omega 2017, 2, 1750−1759

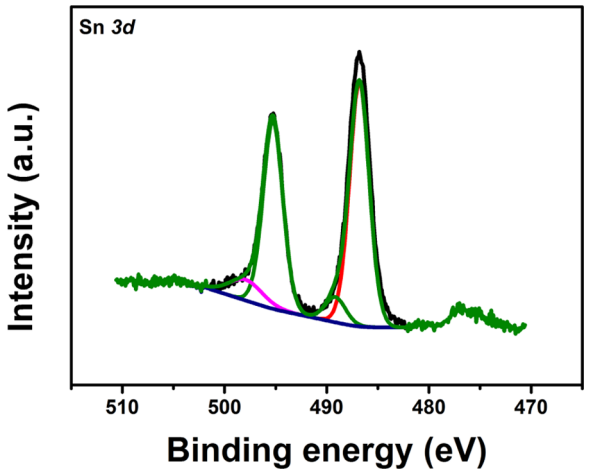

Figure 5. An XPS Sn 3d core-level scan for a sample functionalized with ATBS. The spectrum is dominated by a doublet with a peak-to-peak separation of 8.3 eV. This would suggest the presence of an oxidized Sn species which may be attributed to the low stability of the organostannane monolayer on the surface.

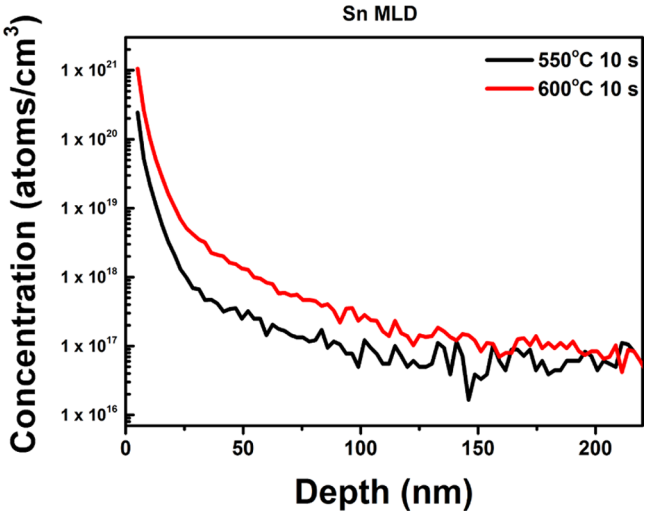

Figure 6. SIMS profile showing concentration vs depth data for ATBS-functionalized samples, which were subjected to a capping step and rapid thermal anneal process. The sample annealed at 550 °C for 10 s exhibited a peak carrier concentration of approximately 2.5 × 10^{20} atoms/cm^3. Another ATBS-functionalized sample similarly treated and annealed at 600 °C exhibited a peak concentration approaching 1.1 × 10^{20} atoms/cm^3.

XPS, despite prolonged sonication in organic solvents post-reaction would imply that ATBS is chemisorbed onto the oxide-free InGaAs surface.

Dopant Characterization of InGaAs Surfaces Functionalized with ATBS and Subsequently Capped and Treated with a Rapid Thermal Anneal. The ABTS-functionalized samples were removed from an inert atmosphere and capped with 50 nm of sputtered SiO_2, and heated in a rapid thermal anneal furnace for 10 s at 550 and 600 °C under nitrogen. The ATBS-functionalized and doped InGaAs samples were tested for the presence of Sn by using Raman scattering before SIMS analysis. Data obtained during Raman scattering are shown in Figure S5. The Raman spectra show a dampening in the intensity of the GaAs-like longitudinal optical mode when compared to those of the bulk, nominally undoped sample. The insets more clearly show the reduction of the GaAs-like and InAs-like longitudinal optical peak. This reduction is due to the creation of charge carrier density as a result of the doping, which causes a decrease of the surface depletion layer. Due to the bulk nature of the material, no damage was observed on the surface of the sample, suggesting that the change in the Raman signature was due to dopant incorporation, as opposed to thermal stress caused by the laser power. As a precaution, a lower laser power of 50% (6 mW) was used. Figure 6 displays a SIMS profile showing concentration versus depth data for the ATBS-functionalized samples, which were subjected to a capping step and rapid thermal anneal process. A significant surface peak was present in both samples with a steep exponential tail. This peak may be attributed to a large amount of Sn located at, or very close to, the surface of the samples within the resolution of the SIMS technique, which is around 5 nm. Samples were sonicated for prolonged periods of time postreaction to ensure all physisorbed material was removed to minimize this surface peak. The junction depths, similar to those of the MPTES-doped samples, were quite deep, approaching 100 nm, highlighting the need for more advanced annealing techniques in order to further optimize the Sn-MLD process.

Stability of MPTES- and ATBS-Functionalized InGaAs Samples toward Reoxidation. The stability that is inferred on semiconductor surfaces by grafted monolayers is interesting for many applications. With respect to device integration, regrowth of surface oxides prior to rapid thermal anneal treatment and other important steps in CMOS processing is undesirable, especially in the moments immediately after a processing step. Surface functionalization greatly increases the oxidation resistance of semiconductor surfaces.[55,56] To ascertain the stability of the MPTES- and ATBS-functionalized samples toward ambient conditions, substrates were left exposed to ambient conditions (air, 20 °C) for periods of time ranging from 24 h to 1 week. Immediately prior to analysis, the samples were rinsed with anhydrous chloroform to remove adventitiously adsorbed material from the surface. The As 3d core-level scan was used to monitor for an increase in oxide formation. Figure 7 shows an overlay of data acquired after 24 h on an MPTES-functionalized sample and an ATBS-functionalized sample. The MPTES-functionalized sample exhibited no evidence of oxide after 24 h. The ATBS-functionalized sample exhibited a presence of oxide near 42 eV after 24 h. The complete acquired stability spectra for the MPTES-functionalized samples are shown in Figure S6a−c. The As 3d core-level data from nonfunctionalized InGaAs substrates are shown in Figure S7a−c. The MPTES-functionalized substrates exhibited excellent resistance toward reoxidation when compared to the nonfunctionalized InGaAs substrates, especially 24 h immediately after functionalization. This stability can be attributed to the tight packing of the MPTES molecule. McGuiness and co-workers also postulated, due to thiol-functionalized III−V compounds showing no observable oxide, that the thiols pack very densely to protect the underlying surface.[57] Additionally, McGuinness suggests that removal of remaining substrate oxides after monolayer formation occurs by a "cleaning" action by the alkanethiol molecules, perhaps involving exchange of S for O at the surface and sacrificial reduction of the inorganic oxides by thiols. Figure S8a−c compares the As 3d XPS spectra for the ATBS-functionalized samples, acquired immediately after preparation and after exposure to ambient conditions for 24 h and 1 week.

DOI: 10.1021/acsomega.7b00204
ACS Omega 2017, 2, 1750−1759

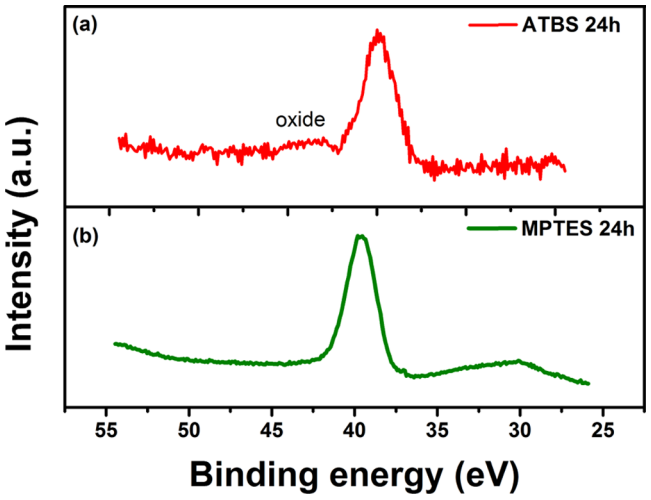

Figure 7. Overlay of data acquired after 24 h from (a) an ATBS-functionalized sample and (b) an MPTES-functionalized sample. The MPTES-functionalized sample exhibited no evidence of oxide after 24 h. The ATBS-functionalized sample exhibited a presence of oxide near 42 eV after 24 h.

These samples exhibited resistance toward oxidation that was not as strong as that of the MPTES-functionalized samples. This may be attributed to the bulky nature of the ATBS molecule where the bulky butyl groups may not allow for as close packing as that of the MPTES molecule. This may cause pinhole oxidation at certain sites on the passivated surface. Efforts were made during the MLD process to ensure strict exclusion of oxygen and moisture. The ATBS sample was exposed to atmospheric conditions for as short a time as possible during transport to the UHV environment of the XPS spectrometer.

CONCLUSIONS

The monolayer doping process has been shown to be a versatile technique for the conformal doping of a range of bulk and nanostructured materials such as Si and Ge. However, reports of MLD on III−V materials are scarce due to the challenging surface chemistry of InGaAs. As III−V materials come to the fore as prime candidates for future CMOS devices, there will be a need to conformally dope such materials whilst ensuring the substrates remain free from oxide ingress. InGaAs can successfully be functionalized with MPTES, a Si containing alkylthiol, as well as ATBS, an organostannane, as shown by XPS analysis. The MPTES-functionalized substrates, in particular, exhibited excellent resistance toward reoxidation, especially within the first 24 h after functionalization, which is advantageous for future integration into CMOS fabrication processes. Raman scattering showed dopant incorporation into the crystal lattice in the case of both MPTES- and ATBS-functionalized substrates when compared to that of a bulk undoped sample. Introduction of Sn via the liquid-phase MLD method proposed in this study could prove beneficial when compared to traditional methods of dopant introduction. Implanting of heavier species into InGaAs, such as Te and Sn, is known to result in amorphization, which needs to be rectified with an anneal step.[58] The Sn-functionalization step outlined in this study avoids the use of highly-energetic ion beams and the resultant damage to the semiconductor crystal lattice. Although junction depths may need to be optimized by using annealing methods with faster ramp up and ramp down rates or more advanced annealing techniques such as laser annealing or flashlamp annealing, SIMS measurements also showed successful dopant diffusion into the substrates with maximum concentrations and depths varying with temperature. Although diffusion of dopants into III−V materials is complex, the surface chemistry developed in this study has potential applications for III−V nanowire devices in a similar manner to strategies applied to silicon and germanium nanowires.[59] Additionally, there are no requirements for gas-phase precursors or complex deposition systems, making this approach suitable and cost-effective for industry.

ASSOCIATED CONTENT

Supporting Information

The Supporting Information is available free of charge on the ACS Publications website at DOI: 10.1021/acsomega.7b00204.

Schematics, XPS stability spectra, SIMS characterization data and additional survey spectra (PDF)

AUTHOR INFORMATION

Corresponding Author

*E-mail: j.holmes@ucc.ie. Tel: +353(0)21 4903608.

Notes

The authors declare no competing financial interest.

ACKNOWLEDGMENTS

We acknowledge financial support from Science Foundation Ireland (Grant: 14/IA/2513). We very much appreciate assistance from Dr. Emanuele Pelucchi and the Epitaxy and the Physics of Nanostructures Group at the Tyndall National Institute for providing InGaAs substrates and for helpful discussions.

REFERENCES

(1) Jones, K. S.; Lind, A. G.; Hatem, C.; Moffatt, S.; Ridgeway, M. C. (Invited) A Brief Review of Doping Issues in III−V Semiconductors. *ECS Trans.* **2013**, *53*, 97−105.

(2) Takagi, S.; Takenaka, M. (Invited) III-V/Ge MOS Transistor Technologies for Future ULSI. *ECS Trans.* **2013**, *54*, 39−54.

(3) del Alamo, J. A. Nanometre-Scale Electronics with III−V Compound Semiconductors. *Nature* **2011**, *479*, 317−323.

(4) Hudait, M. K. (Invited) Heterogeneously Integrated III−V on Silicon for Future Nanoelectronics. *ECS Trans.* **2012**, *45*, 581−594.

(5) Barnett, J.; Hill, R.; Majhi, P. Achieving Ultra-Shallow Junctions in Future CMOS Devices by a Wet Processing Technique. *Solid State Phenom.* **2012**, *187*, 33−36.

(6) Djara, V.; Cherkaoui, K.; Schmidt, M.; Monaghan, S.; O'Connor, E.; Povey, I. M.; O'Connell, D.; Pemble, M. E.; Hurley, P. K. Impact of Forming Gas Annealing on the Performance of Surface-Channel $In_{0.53}G_{0.47}As$ MOSFETs With an ALD Al_2O_3 Gate Dielectric. *IEEE Trans. Electron Devices* **2012**, *59*, 1084−1090.

(7) Eisenbach, A.; Kuphal, E.; Miethe, K.; Hartnagel, H. L. Sn-Doped InGaAs Layers Grown by Low-Pressure Metalorganic Vapour Phase Epitaxy. *J. Cryst. Growth* **1994**, *135*, 129−134.

(8) Collins, G.; Fleming, P.; Barth, S.; O'Dwyer, C.; Boland, J. J.; Morris, M. A.; Holmes, J. D. Alkane and Alkanethiol Passivation of Halogenated Ge Nanowires. *Chem. Mater.* **2010**, *22*, 6370−6377.

(9) Collins, G.; O'Dwyer, C.; Morris, M.; Holmes, J. D. Palladium-Catalyzed Coupling Reactions for the Functionalization of Si Surfaces: Superior Stability of Alkenyl Monolayers. *Langmuir* **2013**, *29*, 11950−11958.

(10) Collins, G.; Holmes, J. D. Chemical Functionalisation of Silicon and Germanium Nanowires. *J. Mater. Chem.* **2011**, *21*, 11052.

DOI: 10.1021/acsomega.7b00204
ACS Omega 2017, 2, 1750−1759

(11) Collins, G.; Fleming, P.; O'Dwyer, C.; Morris, M. A.; Holmes, J. D. Organic Functionalization of Germanium Nanowires Using Arenediazonium Salts. *Chem. Mater.* **2011**, *23*, 1883−1891.
(12) Ho, J. C.; Yerushalmi, R.; Jacobson, Za; Fan, Z.; Alley, R. L.; Javey, A. Controlled Nanoscale Doping of Semiconductors via Molecular Monolayers. *Nat. Mater.* **2008**, *7*, 62−67.
(13) Ho, J. C.; Yerushalmi, R.; Smith, G.; Majhi, P.; Bennett, J.; Halim, J.; Faifer, V. N.; Javey, A. Wafer-Scale, Sub-5 Nm Junction Formation by Monolayer Doping and Conventional Spike Annealing. *Nano Lett.* **2009**, *9*, 725−730.
(14) Ang, K.-W.; Barnett, J.; Loh, W.-Y.; Huang, J.; Min, B.-G.; Hung, P. Y.; Ok, I.; Yum, J. H.; Bersuker, G.; Rodgers, M. et al. In *300 mm FinFET Results Utilizing Conformal, Damage Free, Ultra Shallow Junctions (X_j∼5 nm) Formed with Molecular Monolayer Doping Technique*. 2011 International Electron Devices Meeting; IEEE, 2011; pp 35.5.1−35.5.4.
(15) Voorthuijzen, W. P.; Yilmaz, M. D.; Naber, W. J. M.; Huskens, J.; van der Wiel, W. G. Local Doping of Silicon Using Nanoimprint Lithography and Molecular Monolayers. *Adv. Mater.* **2011**, *23*, 1346−1350.
(16) Hazut, O.; Huang, B.-C.; Pantzer, A.; Amit, I.; Rosenwaks, Y.; Kohn, A.; Chang, C.-S.; Chiu, Y.-P.; Yerushalmi, R. Parallel P-N Junctions across Nanowires by One-Step Ex-Situ Doping. *ACS Nano* **2014**, *8*, 8357−8362.
(17) Longo, R. C.; Cho, K.; Schmidt, W. G.; Chabal, Y. J.; Thissen, P. Monolayer Doping via Phosphonic Acid Grafting on Silicon: Microscopic Insight from Infrared Spectroscopy and Density Functional Theory Calculations. *Adv. Funct. Mater.* **2013**, *23*, 3471−3477.
(18) Ye, L.; Pujari, S. P.; Zuilhof, H.; Kudernac, T.; de Jong, M. P.; van der Wiel, W. G.; Huskens, J. Controlling the Dopant Dose in Silicon by Mixed-Monolayer Doping. *ACS Appl. Mater. Interfaces* **2015**, *7*, 3231−3236.
(19) Ye, L.; González-Campo, A.; Nuñez, R.; de Jong, M. P.; Kudernac, T.; van der Wiel, W. G.; Huskens, J. Boosting the Boron Dopant Level in Monolayer Doping by Carboranes. *ACS Appl. Mater. Interfaces* **2015**, *7*, 27357−27361.
(20) Mathey, L.; Alphazan, T.; Valla, M.; Veyre, L.; Fontaine, H.; Enyedi, V.; Yckache, K.; Danielou, M.; Kerdiles, S.; Guerrero, J.; et al. Functionalization of Silica Nanoparticles and Native Silicon Oxide with Tailored Boron-Molecular Precursors for Efficient and Predictive P -Doping of Silicon. *J. Phys. Chem. C* **2015**, *119*, 13750−13757.
(21) Alphazan, T.; Mathey, L.; Schwarzwälder, M.; Lin, T.-H.; Rossini, A. J.; Wischert, R.; Enyedi, V.; Fontaine, H.; Veillerot, M.; Lesage, A.; et al. Monolayer Doping of Silicon through Grafting a Tailored Molecular Phosphorus Precursor onto Oxide-Passivated Silicon Surfaces. *Chem. Mater.* **2016**, *28*, 3634−3640.
(22) Long, B.; Alessio Verni, G.; O'Connell, J.; Holmes, J.; Shayesteh, M.; O'Connell, D.; Duffy, R. In *Molecular Layer Doping: Non-Destructive Doping of Silicon and Germanium*. 2014 20th International Conference on Ion Implantation Technology (IIT); IEEE, 2014; pp 1−4.
(23) O'Connell, J.; Verni, G. A.; Gangnaik, A.; Shayesteh, M.; Long, B.; Georgiev, Y. M.; Petkov, N.; McGlacken, G. P.; Morris, M. A.; Duffy, R.; Holmes, J. D. Organo-Arsenic Molecular Layers on Silicon for High-Density Doping. *ACS Appl. Mater. Interfaces* **2015**, *7*, 15514−15521.
(24) Duffy, R.; Shayesteh, M.; Thomas, K.; Pelucchi, E.; Yu, R.; Gangnaik, A.; Georgiev, Y. M.; Carolan, P.; Petkov, N.; Long, B.; Holmes, J. D. Access Resistance Reduction in Ge Nanowires and Substrates Based on Non-Destructive Gas-Source Dopant in-Diffusion. *J. Mater. Chem. C* **2014**, *2*, 9248−9257.
(25) O'Connell, J.; Collins, G.; McGlacken, G. P.; Duffy, R.; Holmes, J. D. Monolayer Doping of Si with Improved Oxidation Resistance. *ACS Appl. Mater. Interfaces* **2016**, *8*, 4101−4108.
(26) O'Connell, J.; Biswas, S.; Duffy, R.; Holmes, J. D. Chemical Approaches for Doping Nanodevice Architectures. *Nanotechnology* **2016**, *27*, No. 342002.
(27) Bianco, E.; Butler, S.; Jiang, S.; Restrepo, O. D.; Windl, W.; Goldberger, J. E. Stability and Exfoliation of Germanane: A Germanium Graphane Analogue. *ACS Nano* **2013**, *7*, 4414−4421.
(28) Arduca, E.; Mastromatteo, M.; De Salvador, D.; Seguini, G.; Lenardi, C.; Napolitani, E.; Perego, M. Synthesis and Characterization of P δ -Layer in SiO_2 by Monolayer Doping. *Nanotechnology* **2016**, *27*, No. 075606.
(29) Perego, M.; Seguini, G.; Arduca, E.; Frascaroli, J.; De Salvador, D.; Mastromatteo, M.; Carnera, A.; Nicotra, G.; Scuderi, M.; Spinella, C.; Impellizzeri, G.; Lenardi, C.; Napolitani, E. Thermodynamic Stability of High Phosphorus Concentration in Silicon Nanostructures. *Nanoscale* **2015**, *7*, 14469−14475.
(30) Mastromatteo, M.; Arduca, E.; Napolitani, E.; Nicotra, G.; De Salvador, D.; Bacci, L.; Frascaroli, J.; Seguini, G.; Scuderi, M.; Impellizzeri, G.; Spinella, C.; Perego, M.; Carnera, A. Quantification of Phosphorus Diffusion and Incorporation in Silicon Nanocrystals Embedded in Silicon Oxide. *Surf. Interface Anal.* **2014**, *46*, 393−396.
(31) Adlkofer, K.; Eck, W.; Grunze, M.; Tanaka, M. Surface Engineering of Gallium Arsenide with 4-Mercaptobiphenyl Monolayers. *J. Phys. Chem. B* **2003**, *107*, 587−591.
(32) Yang, G. H.; Zhang, Y.; Kang, E. T.; Neoh, K. G.; Huang, W.; Teng, J. H. Surface Passivation of (100)-Oriented GaAs via Plasma Deposition of an Ultrathin S-Containing Polymer Film and Its Effect on Photoluminescence. *J. Phys. Chem. B* **2003**, *107*, 8592−8598.
(33) Donev, S.; Brack, N.; Paris, N. J.; Pigram, P. J.; Singh, N. K.; Usher, B. F. Surface Reactions of 1-Propanethiol on GaAs(100). *Langmuir* **2005**, *21*, 1866−1874.
(34) Cho, Y.; Ivanisevic, A. Covalent Attachment of TAT Peptides and Thiolated Alkyl Molecules on GaAs Surfaces. *J. Phys. Chem. B* **2005**, *109*, 12731−12737.
(35) Yum, J. H.; Shin, H. S.; Hill, R.; Oh, J.; Lee, H. D.; Mushinski, R. M.; Hudnall, T. W.; Bielawski, C. W.; Banerjee, S. K.; Loh, W. Y.; Wang, W.-E.; Kirsch, P. A Study of Capping Layers for Sulfur Monolayer Doping on III-V Junctions. *Appl. Phys. Lett.* **2012**, *101*, No. 253514.
(36) Kort, K. R.; Hung, P. Y.; Lysaght, P. D.; Loh, W.-Y.; Bersuker, G.; Banerjee, S. Raman Spectroscopy Studies of Dopant Activation and Free Electron Density of $In_{0.53}Ga_{0.47}As$ via Sulfur Monolayer Doping. *Phys. Chem. Chem. Phys.* **2014**, *16*, 6539.
(37) Kort, K. R.; Hung, P. Y.; Loh, W.-Y.; Bersuker, G.; Banerjee, S. Determination of Free Electron Density in Sequentially Doped $In_xGa_{1-x}As$ by Raman Spectroscopy. *Appl. Spectrosc.* **2015**, *69*, 239−242.
(38) Richard D'Costa, V.; Subramanian, S.; Li, D.; Wicaksono, S.; Fatt Yoon, S.; Soon Tok, E.; Yeo, Y.-C. Infrared Spectroscopic Ellipsometry Study of Sulfur-Doped $In_{0.53}Ga_{0.47}As$ Ultra-Shallow Junctions. *Appl. Phys. Lett.* **2014**, *104*, No. 232102.
(39) Subramanian, S.; Kong, E. Y.-J.; Li, D.; Wicaksono, S.; Yoon, S. F.; Yeo, Y.-C. $P_2S_5/(NH_4)_2S_x$-Based Sulfur Monolayer Doping for Source/Drain Extensions in N-Channel InGaAs FETs. *IEEE Trans. Electron Devices* **2014**, *61*, 2767−2773.
(40) Kong, E.; Xiao, G.; Pengfei, G.; Bin, L.; Yee-Chia, Y.In *Novel Technique Comprising Silane Treatment and Laser Anneal for Abrupt Ultra-Shallow Junction Formation for InGaAs N-MOSFETs*, 2013 International Symposium on VLSI Technology, Systems and Application (VLSI-TSA); IEEE, 2013; pp 1−2.
(41) McGuiness, C. L.; Shaporenko, A.; Mars, C. K.; Uppili, S.; Zharnikov, M.; Allara, D. L. Molecular Self-Assembly at Bare Semiconductor Surfaces: Preparation and Characterization of Highly Organized Octadecanethiolate Monolayers on GaAs(001). *J. Am. Chem. Soc.* **2006**, *128*, 5231−5243.
(42) Lie, F. L.; Rachmady, W.; Muscat, A. J. $In_{0.53}Ga_{0.47}As(100)$ Native Oxide Removal by Liquid and Gas Phase HF/H_2O Chemistries. *Microelectron. Eng.* **2010**, *87*, 1656−1660.
(43) Warwick, C. A.; Ono, H.; Kuzuhara, M.; Matsui, J. Amphoteric Doping in Si-Implanted Undoped or In-Doped Czochralski GaAs. *Jpn. J. Appl. Phys.* **1987**, *26*, L1398−L1400.

DOI: 10.1021/acsomega.7b00204
ACS Omega 2017, 2, 1750−1759

(44) Bahl, M. K.; et al. Relaxation during Photoemission and LMM Auger Decay in Arsenic and Some of Its Compounds. *J. Chem. Phys.* **1976**, *64*, 1210.
(45) Epp, J. M.; Dillard, J. G. Effect of Ion Bombardment on the Chemical Reactivity of Gallium arsenide(100). *Chem. Mater.* **1989**, *1*, 325−330.
(46) Shaporenko, A.; Adlkofer, K.; Johansson, L. S. O.; Ulman, A.; Grunze, M.; Tanaka, M.; Zharnikov, M. Spectroscopic Characterization of 4′-Substituted Aromatic Self-Assembled Monolayers on GaAs(100) Surface. *J. Phys. Chem. B* **2004**, *108*, 17964−17972.
(47) Hernández, S.; Marcos, B.; Cuscó, R.; Blanco, N.; González-Díaz, G.; Artús, L. Lattice Damage Study of Implanted InGaAs by Means of Raman Spectroscopy. *J. Lumin.* **2000**, *87*−*89*, 721−723.
(48) Hernández, S.; Blanco, N.; Mártil, I.; González-Díaz, G.; Cuscó, R.; Artús, L. Evidence of Phosphorus Incorporation into InGaAs/InP Epilayers after Thermal Annealing. *J. Appl. Phys.* **2003**, *93*, 9019.
(49) Aldridge, H. L.; Lind, A. G.; Law, M. E.; Hatem, C.; Jones, K. S. Concentration-Dependent Diffusion of Ion-Implanted Silicon in $In_{0.53}Ga_{0.47}As$. *Appl. Phys. Lett.* **2014**, *105*, No. 042113.
(50) Lind, A. G.; Aldridge, H. L.; Bomberger, C. C.; Hatem, C.; Zide, J. M. O.; Jones, K. S. Annealing Effects on the Electrical Activation of Si Dopants in InGaAs. *ECS Trans.* **2015**, *66*, 23−27.
(51) Wündisch, C.; Posselt, M.; Schmidt, B.; Heera, V.; Schumann, T.; Mücklich, a; Grötzschel, R.; Skorupa, W.; Clarysse, T.; Simoen, E.; Hortenbach, H. Millisecond Flash Lamp Annealing of Shallow Implanted Layers in Ge. *Appl. Phys. Lett.* **2009**, *95*, No. 252107.
(52) Prucnal, S.; Sun, J. M.; Muecklich, A.; Skorupa, W. Flash Lamp Annealing vs Rapid Thermal and Furnace Annealing for Optimized Metal-Oxide-Silicon-Based Light-Emitting Diodes. *Electrochem. Solid-State Lett.* **2007**, *10*, H50.
(53) Colin, A.; Morin, P.; Beneyton, R.; Pinzelli, L.; Mathiot, D.; Fogarassy, E. Dopant Diffusion and Activation Induced by Sub-Melt Laser Anneal within the Co-Implanted P+ Polycrystalline Silicon Gate Used in CMOS Technologies. *Thin Solid Films* **2010**, *518*, 2390−2393.
(54) Nguyen, N. D.; Rosseel, E.; Takeuchi, S.; Everaert, J.-L.; Yang, L.; Goossens, J.; Moussa, A.; Clarysse, T.; Richard, O.; Bender, H.; Zaima, S.; Sakai, A.; Loo, R.; Lin, J. C.; Vandervorst, W.; Caymax, M. Use of P- and N-Type Vapor Phase Doping and Sub-Melt Laser Anneal for Extension Junctions in Sub-32 nm CMOS Technology. *Thin Solid Films* **2010**, *518*, S48−S52.
(55) Sieval, A. B.; Linke, R.; Zuilhof, H.; Sudhölter, E. J. R. High-Quality Alkyl Monolayers on Silicon Surfaces. *Adv. Mater.* **2000**, *12*, 1457−1460.
(56) Cai, Q.; Xu, B.; Ye, L.; Di, Z.; Huang, S.; Du, X.; Zhang, J.; Jin, Q.; Zhao, J. 1-Dodecanethiol Based Highly Stable Self-Assembled Monolayers for Germanium Passivation. *Appl. Surf. Sci.* **2015**, *353*, 890−901.
(57) Mcguiness, C. L.; Shaporenko, A.; Zharnikov, M.; Walker, A. V.; Allara, D. L. Molecular Self-Assembly at Bare Semiconductor Surfaces: Investigation of the Chemical and Electronic Properties of the Alkanethiolate-GaAs(001) Interface. *J. Phys. Chem. C* **2007**, *111*, 4226−4234.
(58) Zhang, G. L.; Mo, D.; Liang, Z. N.; Niesen, L. Impurity Lattice Sites after Implantation of Te and Sb in GaAs: Search for the DX Centre. *Hyperfine Interact.* **1990**, *56*, 1661−1665.
(59) Long, B.; Alessio Verni, G.; O'Connell, J.; Shayesteh, M.; Gangnaik, A.; Georgiev, Y. M.; Carolan, P.; O'Connell, D.; Kuhn, K. J.; Clendenning, S. B.; Nagle, R.; Duffy, R.; Holmes, J. D. Doping Top-down E-Beam Fabricated Germanium Nanowires Using Molecular Monolayers. *Mater. Sci. Semicond. Process.* **2017**, *62*, 196−200.

DOI: 10.1021/acsomega.7b00204
ACS Omega 2017, 2, 1750−1759